Influence of the driving rate in a two-dimensional rice pile model

Kinga A. Lőrincz and Rinke J. Wijngaarden

Division of Physics and Astronomy, Faculty of Sciences, Vrije Universiteit, De Boelelaan 1081, 1081HV Amsterdam, The Netherlands

We study the influence of the driving rate in the two-dimensional Oslo rice pile model. We find that the usual power-law behavior of the avalanche size distribution still holds for small avalanches, independent of the driving rate. The signature of fast driving is, however, the increase of the incidence rate of large avalanches. For larger driving rates, this increase is more prominent and spreads to smaller avalanche sizes. As a result, the mass flow due to large avalanches is increased much more than would be expected from an increase in driving rate alone. Fast driving leads to a dramatic increase in devastating avalanches, just before the continuous flow regime is reached.

I. INTRODUCTION

Self-organized criticality (SOC) [1] was introduced as a unifying theory for many systems in nature and society: snow avalanches [2], earthquakes [3], stock markets [4], forest fires [5], and biological evolution [6]. One of the common features of these systems is a power-law distribution of the event sizes. However, these systems are difficult to study experimentally, so numerical models were developed that exhibit the same statistical behavior. A couple of the models that are thought to exhibit SOC behavior are the Bak-Tang-Wiesenfeld (BTW) sandpile model [1,7], the rice pile models (the Oslo model [8] and the Amaral-Lauritsen [9] model), and the forest fire models (the Drossel-Schwabl [10] and the Bak-Chen-Tang [11] models; see, however, also [12]).

An important prerequisite to obtain SOC is slow driving, i.e., the time scale of the driving should be much larger than the lifetime of an event. However, in most experimental systems it is difficult to estimate what slow driving means quantitatively. Therefore a good understanding of the response of the system to different driving rates is needed. Tang *et al.* [13] studied how the average height of the pile changes with different driving rates in the BTW sand pile model. Corral *et al.* [14] studied the transition from the avalanche phase to the continuous flow regime in the one-dimensional Oslo rice pile model [8]. They found that the roughness exponent of the pile does not change as the driving rate of the system is increased, provided that the pile is in the avalanche regime. If the driving rate is further increased, such that the continuous flow phase is reached, the root mean square of height fluctuations becomes smaller and is independent of the system size. In addition, the transit time and the average slope of the pile as a function of driving rate are power laws, with exponents dependent on the phase the pile is in. Interestingly, the exponents that characterize the continuous flow regime are connected to the critical exponents that describe the avalanches in the SOC limit. However, the effect of the driving rate on the distribution of avalanche sizes was not studied. Malamud *et al.* [5] studied the distribution of forest fires and showed that the forest fire model displays the same SOC behavior as real wild fires. They have performed simulations with three different sparking rates and found a power-law distribution of the burned areas with exponents dependent on the sparking rates.

In this paper we study the influence of the driving rate on the distribution of avalanche sizes for the Oslo rice pile model generalized to two dimensions. We chose this particular system because its dynamics is closest to a three-dimensional experimental rice pile [15]. We find that the distribution of avalanche sizes is a power law for all driving rates in the small avalanche regime. However, due to the merging of avalanches at higher driving rates, a hump appears in the large avalanche regime. This hump influences also the apparent exponent of the distribution of avalanche sizes.

A detailed description of the model with the parameters used can be found in Sec. II. In Sec. III we present our results, and in Sec. IV we draw our conclusions.

II. NUMERICAL SIMULATIONS

For our simulations we use the Oslo [8] rice pile model generalized to two dimensions [16] in a similar manner as the two-dimensional BTW sand pile model [1,7].

The system consists of an $L \times L$ square lattice. The value at each site (i,j) of the lattice represents the slope $z(i,j)$ of the pile in that point. The "particles" in this model are the slope units. Particles are always deposited along the row $y=1$ at the closed boundary. If locally the slope of the pile exceeds the critical slope $z_c(i,j)$ an avalanche is started and the following relaxation rules are applied:

$$z(i,j) \mapsto z(i,j) - 4,$$

$$z(i \pm 1, j) \mapsto z(i \pm 1, j) + 1,$$

$$z(i, j \pm 1) \mapsto z(i, j \pm 1) + 1. \tag{1}$$

This event is called a toppling (note: for a two-dimensional lattice, the heights cannot be derived from the slopes). All the sites that are selected for toppling are identified and updated simultaneously (matrix update step). The system has closed boundaries at $x=1$, $x=L$, and $y=1$ and an open boundary at $y=L$. If the critical slope is exceeded at a site at a closed boundary, the slope is decreased by three units (in the corner between two closed boundaries, by two units), which are evenly distributed between the three (or two) neighbors
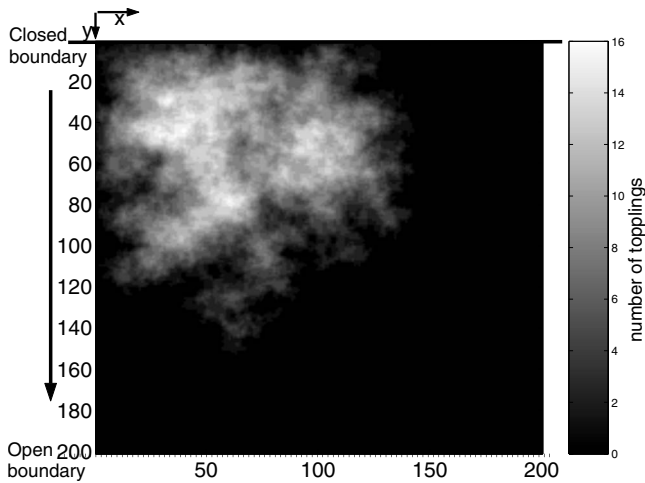
FIG. 1. Image of an avalanche obtained using the Oslo rice pile model on a 200×200 lattice, with a driving rate of $r=0$. The avalanche propagates from the top to the bottom, from the closed boundary to the open one, along the direction indicated by the arrow. The color coding (see the right-hand side scale bar) indicates the number of topplings that occurred at each site.

in the pile. If the critical slope is exceeded at an open boundary, the rules (1) are applied; however, the slope unit that falls off the pile is lost. Particles are always deposited along the row $y=1$ at the closed boundary. The value of the critical slope is chosen randomly to be $z_c(i,j)=3$ or $z_c(i,j)=4$. This randomness of the critical slope reflects the different ways an anisotropic rice grain can fall. After a toppling event the critical slope of the site (i,j) that was relaxed is updated, $z_c(i,j) \in \{3,4\}$. The avalanche propagates until all the sites in the system are stable, $z(i,j) \leq z_c(i,j)$ for $i,j \in [1,L]$. Note that thus all avalanches that occur on the pile are included in the analysis.

The feeding of the pile is continuous; particles are added also during the evolution of the avalanches. The driving rate is defined as $r=1/\Delta t$ [14], where Δt is the number of matrix updates between depositions, so at every Δt step one particle is deposited at a random site of the row $y=1$. $r \rightarrow 0$ is the SOC limit, when one particle is added only between the avalanches. This is henceforth denoted by $r=0$.

The response of the system to the newly deposited particles is avalanches of all sizes. Figure 1 shows an image of an avalanche on a 200×200 lattice, obtained with a driving rate of $r=0$. The avalanche propagates from the top to the bottom, from the closed to the open boundary. After each site is stable we identify the individual avalanche clusters. The size of the avalanche clusters, s, is defined as the number of topplings in each cluster.

III. INFLUENCE OF THE DRIVING RATE ON THE DISTRIBUTION OF AVALANCHE SIZES

In this section we present the results of the numerical simulations. The simulations consist of at least 10^5 avalanches (unless stated otherwise). The larger the system, the larger the maximum avalanche size observed in the simulation is. However, large avalanches are less frequent than
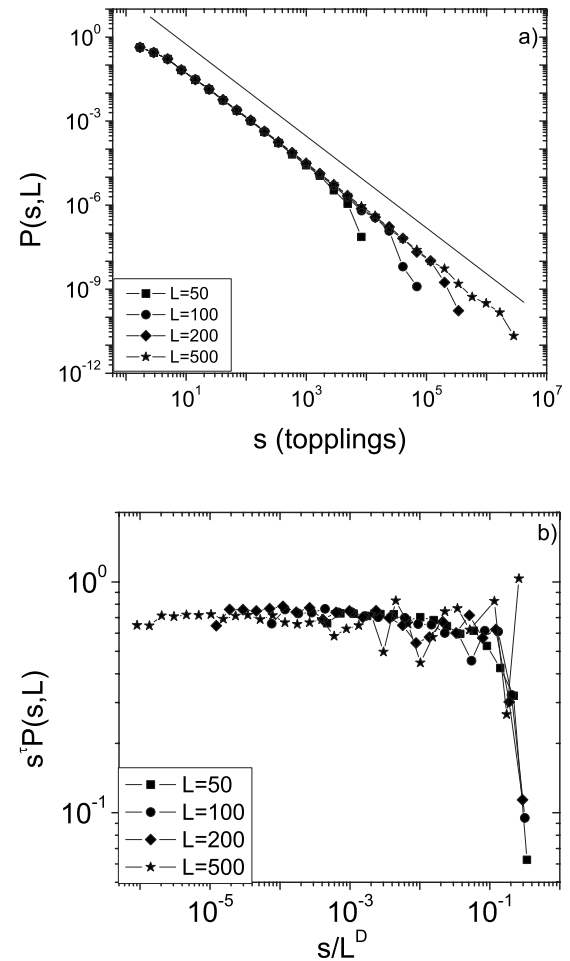

FIG. 2. (a) Distribution of avalanche sizes in the slow driving regime ($r=0$) for systems with linear sizes $L=50$, 100, 200, and 500. The distributions are power laws over up to five orders of magnitude with an exponent $\tau=1.63$. The straight line is a fit to the data for $L=500$ and shifted for clarity. (b) The same data scaled to obtain a data collapse. The values used for the scaling are $D=2.55$ and $\tau=1.63$.

small ones, so more time steps are needed to obtain reliable statistics in the large avalanche regime. Hence, larger systems require the collection of more avalanches.

We have performed simulations with different driving rates $r \in \{0, 0.1, 0.2, 0.25, 0.33, 0.5, 1, 1.5, 2\}$. Even with the highest driving rate used, the system displayed intermittent avalanches, i.e., the continuous flow regime [14] was not yet reached. For $r=4$, which means that four particles are randomly added along the first row of the system at each matrix update step, the continuous flow regime is reached in the system with linear size $L=50$. We say that the system is in the continuous flow if the first avalanche does not stop in 10^7 matrix update steps. Although we still observe individual avalanches for the driving rate $r=3$, the lifetime of the avalanches is greatly increased, so it is difficult to obtain reliable statistics in this case.

In Fig. 2(a) we present the distribution of avalanche sizes in the slow driving regime ($r=0$), for systems with linear sizes: $L=50$, 100, 200, and 500. The distributions are power laws for up to five orders of magnitude: $P(s) \sim s^{-\tau}$, with an
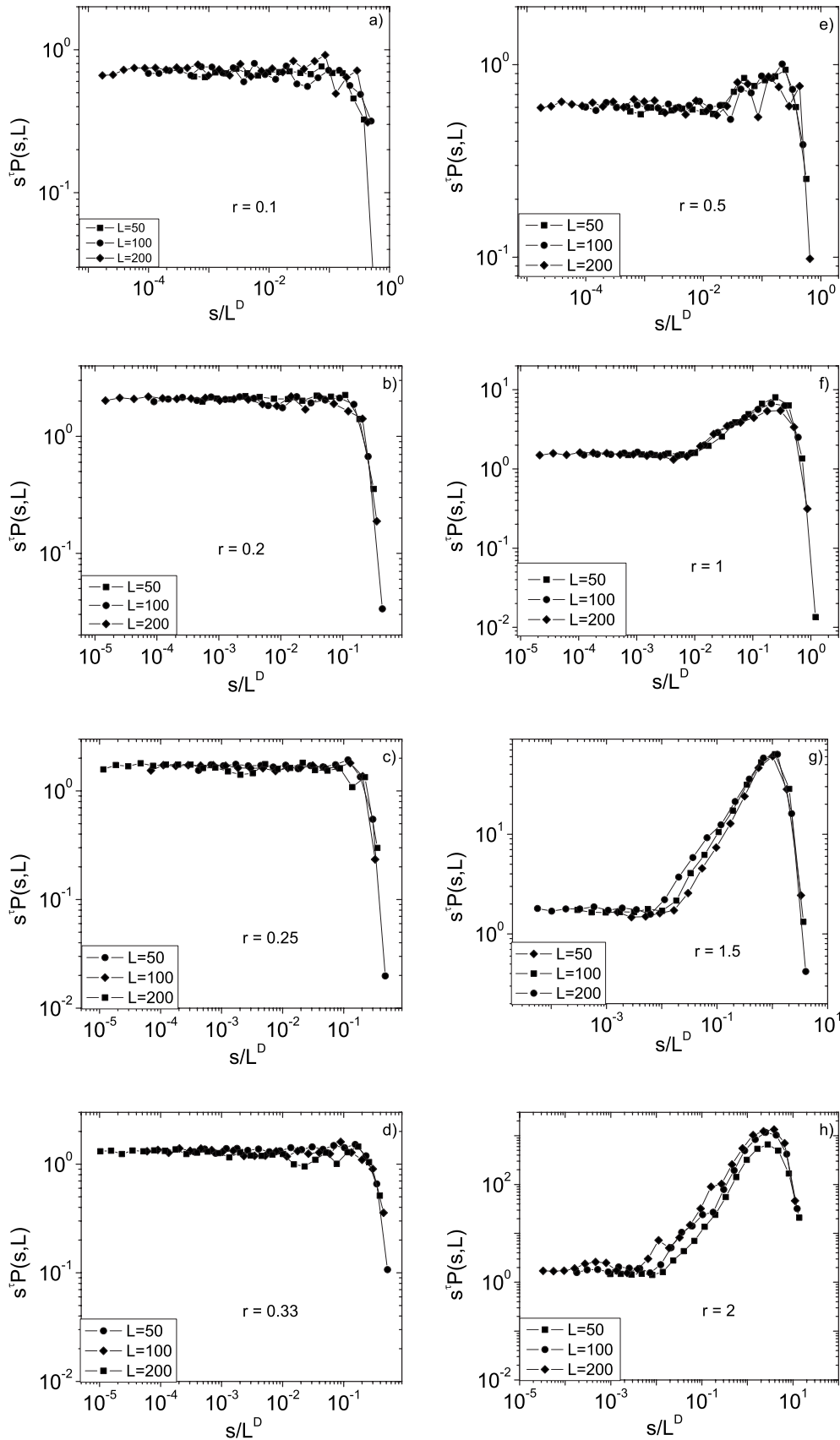
FIG. 3. Finite size scaling of the avalanche sizes for driving rates r as indicated. The parameters used for the data collapse are: (a) D $=2.65$ and $\tau=1.64$, (b) $D=2.59$ and $\tau=1.63$, (c) $D=2.55$ and $\tau=1.62$, (d) $D=2.55$ and $\tau=1.60$, (e) $D=2.53$ and $\tau=1.59$, (f) $D=2.55$ and $\tau=1.53$, (g) $D=2.40$ and $\tau=1.55$, and (h) $D=2.45$ and $\tau=1.63$.
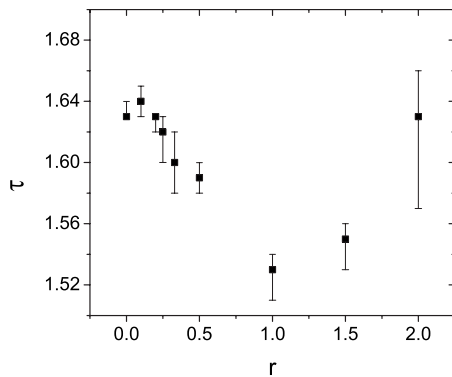
FIG. 4. Dependence of the exponent τ, as obtained from finite size scaling, on the driving rate r. The error bars indicate the range of values obtained from a power-law fit of the avalanche size distribution for different system sizes.

exponent $\tau = 1.63$. The deviation from the power law in the large avalanche regime is a finite size effect. However, a more reliable way to determine the exponent τ of the distribution is by means of finite size scaling. For $r = 0$, the best data collapse is obtained using the parameters $\tau = 1.63$ and $D = 2.55$ [see Fig. 2(b)]. Here D is the fractal dimension of the avalanches; however, D was determined from optimizing the data collapse in Fig. 2(b).

For higher driving rates, we have performed simulations on systems with linear sizes: $L = 50$, 100, and 200. The distribution of avalanche sizes is a power law for all driving rates in the small avalanche regime. For each value of r we can obtain the exponent of the distribution by collapsing the data for the different system sizes L (see Fig. 3). In the interval $r \in [0.2, 1]$ we observe an apparent decrease of the exponent τ, from 1.63 to 1.53, with increasing driving rates (see Fig. 4), while a hump starts to appear in the large avalanche regime. This is due to the fact that adding particles to the already unstable pile initiates several simultaneous avalanches which can merge. This means that the probability to have large avalanches increases, thereby creating a hump in

the large avalanche regime. If the driving rate is increased even further, $r > 1$, meaning that we add more than one particle at each matrix update step, the hump becomes the dominant feature of the distribution. However, the small avalanches are still power-law distributed. The seemingly continuously changing τ with increasing driving rate is a behavior unexpected for a critical exponent. However, the apparent fluctuation of the exponent is probably caused by the presence of the hump in the large avalanche regime and therefore is not significant.

The volume fractal dimension D of the avalanches seems to decrease and the avalanches become less compact if the driving rate is increased ($r > 1$). However, the hump in this case does not collapse nicely for the different system sizes [Figs. 3(f)–3(h)], so it is difficult to estimate the value of D precisely from the finite size scaling procedure.

IV. CONCLUSIONS

We have studied the influence of the driving rate on the distribution of avalanche sizes. We find that the signature of fast driving is the appearance of a hump in the large avalanche regime. This hump is more and more pronounced as the feeding rate increases. However, the distribution of small avalanche sizes remains a power law independent of driving rate. The apparent value of the exponent of this distribution is influenced by the presence of the hump. The apparent change of the power-law exponents in our system as a function of the driving rate could explain the different exponents found for real forest fires in different regions [5], but also the slight variations in the exponents for the snow avalanches in different areas [2]. In many natural systems it is impossible to change the driving rate, but in the laboratory experiments [e.g., a one-dimensional rice pile [17] and a three-dimensional rice pile [15] (both using long grain rice), a one-dimensional pile of steel balls [18]] it is worthwhile to experiment with different feeding rates, to verify whether the system is driven in the SOC limit or not.

[1] P. Bak, C. Tang, and K. Wiesenfeld, Phys. Rev. Lett. **59**, 381 (1987).

[2] K. Birkeland and C. Landry, Geophys. Res. Lett. **29**, 1554 (2002).

[3] P. Bak, K. Christensen, L. Danon, and T. Scanlon, Phys. Rev. Lett. **88**, 178501 (2002); A. Sornette and D. Sornette, Europhys. Lett. **9**, 197 (1989); J. Carlson, J. Langer, and B. Shaw, Rev. Mod. Phys. **66**, 657 (1994).

[4] J. Scheinkman and M. Woodford, Am. Econ. Rev. **84**, 417 (1994); P. Bak, K. Chen, J. Scheinkman, and M. Woodford, Ric. Econ. **47**, 3 (1993).

[5] B. Malamud, G. Morein, and D. Turcotte, Science **281**, 1840 (1998).

[6] J. Bascompte and R. V. Solé, Trends Ecol. Evol. **10**, 361 (1995); H. Flyvbjerg, K. Sneppen, and P. Bak, Phys. Rev. Lett. **71**, 4087 (1993); S. A. Kauffman and S. Johansen, J. Theor. Biol. **149**, 467 (1991).

[7] P. Bak, C. Tang, and K. Wiesenfeld, Phys. Rev. A **38**, 364 (1988).

[8] K. Christensen, A. Corral, V. Frette, J. Feder, and T. Jøssang, Phys. Rev. Lett. **77**, 107 (1996).

[9] L. A. Nunes Amaral and K. B. Lauritsen, Phys. Rev. E **54**, R4512 (1996).

[10] B. Drossel and F. Schwabl, Phys. Rev. Lett. **69**, 1629 (1992).

[11] P. Bak, K. Chen, and C. Tang, Phys. Lett. A **147**, 297 (1990).

[12] P. Grassberger and H. Kantz, J. Stat. Phys. **63**, 685 (1991); G. Pruessner and H. J. Jensen, Phys. Rev. E **65**, 056707 (2002); P. Grassberger, New J. Phys. **4**, 17 (2002).

[13] C. Tang and P. Bak, Phys. Rev. Lett. **60**, 2347 (1988).

[14] A. Corral and M. Paczuski, Phys. Rev. Lett. **83**, 572 (1999).

[15] K. A. Lőrincz and R. J. Wijngaarden, Phys. Rev. E **76**, 040301(R) (2007).

[16] C. M. Aegerter, Physica A **319**, 1 (2003).

[17] V. Frette, K. Christensen, A. Malthe-Sørenssen, J. Feder, T. Jøssang, and P. Meakin, Nature (London) **379**, 49 (1996).

[18] E. Altshuler, O. Ramos, C. Martinez, L. E. Flores, and C. Noda, Phys. Rev. Lett. **86**, 5490 (2001).